SOX9 and TCF transcription factors associate to mediate Wnt/β-catenin target gene activation in colorectal cancer

Aravinda-Bharathi Ramakrishnan, Peter E. Burby, Kavya Adiga[iD]**, and Ken M. Cadigan**[*][iD]

From the Department of Molecular, Cellular, and Developmental Biology, University of Michigan, Ann Arbor, Michigan, USA

Edited by Brian Strahl

Activation of the Wnt/β-catenin pathway regulates gene expression by promoting the formation of a β-catenin–T-cell factor (TCF) complex on target enhancers. In addition to TCFs, other transcription factors interact with the Wnt/β-catenin pathway at different levels to produce tissue-specific patterns of Wnt target gene expression. The transcription factor SOX9 potently represses many Wnt target genes by downregulating β-catenin protein levels. Here, we find using colony formation and cell growth assays that SOX9 surprisingly promotes the proliferation of Wnt-driven colorectal cancer (CRC) cells. In contrast to how it indirectly represses Wnt targets, SOX9 directly co-occupies and activates multiple Wnt-responsive enhancers in CRC cells. Our examination of the binding site grammar of these enhancers shows the presence of TCF and SOX9 binding sites that are necessary for transcriptional activation. In addition, we identify a physical interaction between the DNA-binding domains of TCFs and SOX9 and show that TCF-SOX9 interactions are important for target gene regulation and CRC cell growth. Our work demonstrates a highly context-dependent effect of SOX9 on Wnt targets, with the presence or absence of SOX9-binding sites on Wnt-regulated enhancers determining whether they are directly activated or indirectly repressed by SOX9.

Transcriptional regulation by the Wnt/β-catenin pathway is essential for metazoan development and homeostasis (1), and the transcription factors (TFs) of the T-cell factor/lymphoid enhancer factor family (TCF/LEF family or TCFs) are major effectors of this signaling cascade (2). Clusters of TCF-binding sites are characteristic of many Wnt-regulated elements (WREs), the *cis*-regulatory DNA elements that drive Wnt-responsive transcription (3). WRE activation is triggered by the Wnt-dependent stabilization and accumulation of the protein β-catenin, which is recruited to WREs by TCFs. β-catenin recruits coactivators to induce Wnt target gene transcription (2, 4). Signaling by Wnt proteins performs many essential developmental functions that do not involve transcriptional regulation through β-catenin (5, 6). For brevity, we use the phrases "Wnt signaling" and "Wnt target gene" in this study to refer to Wnt signaling through β-catenin and genes regulated by the Wnt/β-catenin pathway.

While TCFs mediate Wnt target gene activation across cell types, there is great spatiotemporal diversity in the identity of Wnt target genes, with different tissues expressing unique cell type–specific Wnt transcriptional programs. This specificity is thought to arise from interactions between TCFs and other TFs that help determine cell fate and identity. Many non-TCF TFs bind to WREs and affect Wnt target gene expression, but a comprehensive molecular understanding of how these TFs generate target gene specificity is still incomplete (7, 8). One well-studied example is TFs of the CDX family, which bind to several WREs and recruit TCFs to them (9, 10). Their ability to form complexes with TCFs is essential for the activation of several Wnt target genes (11).

Another group of developmentally important TFs that modulate Wnt target gene expression is the SOX family of proteins. While some SOX family members directly bind to TCFs and β-catenin and promote the expression of specific Wnt targets (12–15), other SOX proteins are known to repress Wnt/β-catenin signaling, with SOX9 being the most intensively studied. SOX9 has essential functions in the development of cartilage and the skeletal system, and mutations in SOX9 are associated with sex reversal and severe skeletal deformities in humans (16, 17). SOX9 is also well known for its role in promoting testis formation during mammalian development (18). Genetic studies have shown that testis or ovary commitment in mammalian gonadal development involves a mutual opposition between the Wnt/β-catenin pathway, which promotes ovarian development and inhibits testis fate, and SOX9, which inhibits the Wnt/β-catenin pathway to promote testes growth (19). In several different mammalian cell lines, the overexpression of SOX9 causes a reduction in Wnt transcriptional readouts and in β-catenin protein levels (20–23). Recent work from our group found that SOX9 promoted β-catenin degradation by transcriptionally activating the Notch pathway coactivator MAML2, which associates with β-catenin (22).

Although primarily characterized as a repressor of Wnt/β-catenin target genes, correlative evidence hints at a more complex relationship between SOX9 and Wnt/β-catenin signaling in the intestinal epithelium and in colorectal cancer (CRC). The villi of the intestinal epithelium consist of short lived terminally differentiated cells that are continuously replenished from a population of intestinal epithelial stem cells. The proliferation of these stem cells and the differentiation of the Paneth cells, which surround and metabolically

* For correspondence: Ken M. Cadigan, cadigan@umich.edu.

support them, are both dependent on Wnt/β-catenin signaling (24, 25). Paneth cells express high levels of SOX9 (26), and the loss of either SOX9 or Wnt signaling prevents Paneth cell differentiation (24, 27, 28). Additionally, SOX9 overexpression in Wnt-dependent CRC lines induces the expression of many genes characteristic of Paneth cells (29). Some of these are also directly activated by Wnt signaling (29–31), suggesting the possibility of SOX9 and Wnt signaling working together to activate gene expression. Understanding the relationship between SOX9 and Wnt signaling in this context requires an understanding of the regulatory logic of target gene WREs regulated by both factors.

Aberrant Wnt/β-catenin pathway activation in intestinal stem cells leads to uncontrolled proliferation, and consequently, activating mutations in the Wnt/β-catenin pathway are major drivers of CRC (4, 32). Additionally, mutations that increase the activity of WREs that regulate oncogenes such as *MYC* are also associated with increased cancer risk (33–36). Many Wnt-dependent CRC lines and primary CRC samples also show high levels of SOX9 expression (37, 38), and recent reports suggest that SOX9 promotes stemness and survival of some CRC lines (29, 39, 40). The findings of SOX9 promoting Paneth cell fate and CRC cell survival are at odds with models of SOX9 as a Wnt/β-catenin pathway repressor.

In this study, we interrogate the relationship between SOX9 and Wnt signaling in regulating gene expression. In contrast to its previously known role as a repressor of Wnt/β-catenin signaling, we show that SOX9 and Wnt signaling work together to promote the growth and survival of CRC cells. Among the target genes activated by Wnt/β-catenin signaling and SOX9 is the oncogene *MYC*. In CRC cells, SOX9 is associated with many WREs, including several cancer risk-associated enhancers of *MYC*. Our characterization of the *cis*-regulatory grammar that allows SOX9 to activate Wnt target genes reveals the presence of SOX9-binding sites in the c-*myc*-335 WRE, which regulate enhancer activity along with TCF sites. A similar regulatory logic is also seen in the promoters of *Defa5* and *Defa6*, two markers of Paneth cells, that are synergistically upregulated under high Wnt, high SOX9 conditions. With reporter mutagenesis and synthetic reporters, we show that the combination of TCF- and SOX-binding sites is necessary and sufficient for synergistic activation by Wnt and SOX9. Mechanistically, we show that SOX9 directly binds to TCFs. Through a novel SOX9 separation-of-function mutant that is defective in TCF binding, we show that the activation of WREs and CRC cell growth both require not just the activities of TCFs and SOX9 but also the activity of a TCF-SOX9 complex. Our work demonstrates that in addition to its role as a repressor of the Wnt/β-catenin pathway, SOX9 works together with the Wnt/β-catenin pathway to activate a subset of Wnt target genes.

Results

Both SOX9 and Wnt signaling promote the growth and survival of CRC cells

To explore the roles of SOX9 and Wnt/β-catenin signaling in CRC, we tested the consequences of depleting SOX9 and/or

β-catenin in LS174T CRC cells. These cells contain an activating mutation in β-catenin (S45F) and are dependent on Wnt signaling for their growth and survival (41, 42). We used LS174T cells containing a doxycycline (DOX)-inducible β-catenin shRNA expression cassette (41) (referred to as LS174T-pTER-β-cat cells) and transduced them with constructs expressing either nontargeting (Scrambled) or SOX9-targeting shRNAs (Table S1). Western blots showed reduced SOX9 expression in the two SOX9 shRNA lines (Fig. 1A, lanes 2,3). This reduction of SOX9 protein levels was not accompanied by an upregulation of β-catenin protein, as would be expected if SOX9 was promoting β-catenin turnover (Fig. 1A, lanes 2,3). This suggested that SOX9 does not repress β-catenin levels in these cells. SOX9 protein levels were not affected by β-catenin depletion, suggesting that SOX9 is not a target of Wnt signaling in these cells (Fig. 1A, lanes 1,4).

To understand whether SOX9 and Wnt signaling worked together to promote the survival of LS174T-pTER-β-cat cells, we tested for a SOX9 requirement in a colony formation assay with and without DOX-induced β-catenin depletion. Knocking down SOX9 alone resulted in fewer colonies, and the combined depletion of β-catenin and SOX9 reduced the clonogenicity of these cells even further (Fig. 1, B and C). We then tested the impact of Wnt signaling and SOX9 on the growth rate of these cells. We treated cells with or without DOX for 48 h and measured metabolic activity as a proxy for cell number using an 3-(4,5-dimethylthiazol-2-yl)-2,5-diphenyltetrazolium bromide (MTT) assay. The depletion of β-catenin or SOX9 led to slower growth, and combined depletion of β-catenin and SOX9 reduced growth 4- to 5-fold (Fig. 1D). To ensure that our findings were not specific to LS174T cells, we also tested the role of SOX9 in promoting the survival of DLD-1 cells. DLD-1 cells also have elevated levels of Wnt signaling, but unlike LS174T cells, express a WT β-catenin protein and a truncated form of the destruction complex component APC (43). In DLD-1 cells, SOX9 depletion caused a 3-fold reduction in colony formation (Fig. 1, E and F). Just like in LS174T cells, SOX9 depletion did not cause an upregulation of β-catenin protein levels, and the inhibition of Wnt signaling through a dominant negative TCF (dnTCF) construct (44) did not reduce SOX9 protein levels (Fig. S1A).

We then examined the importance of Wnt signaling and SOX9 across a panel of CRC lines using data from the Cancer Cell Line Encyclopedia (CCLE) (45, 46). First, we examined gene expression data and correlated it with dependency scores calculated from CRISPR KO experiments using the Chronos algorithm (47). As expected in CRC, 49/53 lines examined showed high β-catenin (*CTNNB1*) expression and dependence based on our cutoffs (Fig. S1B). A similar analysis for SOX9 revealed that 38/53 lines showed high SOX9 expression and SOX9-dependent growth (Fig. S1C). Dependence on SOX9 was highly correlated with β-catenin-dependence, with 40/56 lines being highly dependent on both β-catenin and SOX9 (Fig. S1D). As a negative control, we looked at SOX17, which represses Wnt targets and inhibits the proliferation of CRC cells (13). Just 2/56 lines showed a dependence on both genes (Fig. S1E). Across all cancers in the CCLE database (n = 1070), β-catenin
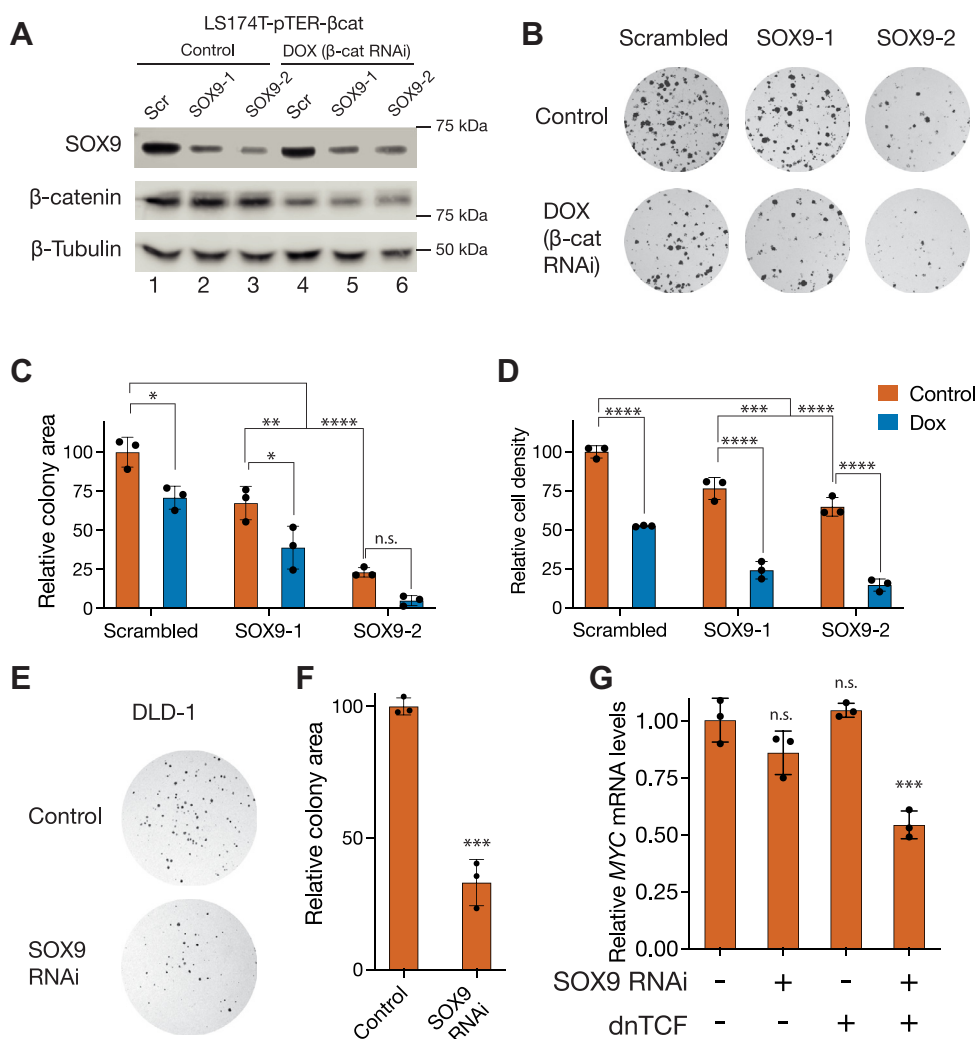
Figure 1. Wnt signaling and SOX9 work together to promote the growth and proliferation of colorectal cancer cells. *A*, Western blots showing depletion of SOX9 and β-catenin in LS174T colorectal cancer cells by RNAi. Cells were stably transduced with constructs expressing either a scrambled (Scr) or two independent SOX9-targeting shRNAs (SOX9-1, SOX9-2) and then treated with DOX for 24 h to deplete β-catenin. *B*, representative images showing reduced colony formation in LS174T cells after knockdown of SOX9 and β-catenin. Cells were treated in similar conditions as in (*A*) and then seeded at a density of 1000 cells/well. *C*, quantification of the area occupied by the colonies shown in (*B*). *D*, RNAi against β-catenin and SOX9 reduces the growth rate of LS174T cells. Cells were treated with DOX for 48 h, following which relative cell numbers were measured using an MTT assay. *E*, reduced colony formation in DLD-1 colorectal cancer cells after SOX9 knockdown. Cells were transfected with either a control plasmid or one expressing a SOX9 targeting shRNA and plated at a density of 500 cells/well. *F*, quantification of the area occupied by the colonies shown in (*E*). *G*, RT-qPCR data showing *MYC* mRNA levels in DLD-1 cells after transfection with plasmids expressing dominant negative TCF (dnTCF), SOX9 RNAi, or both. mRNA levels were measured with RT-qPCR 24 h after transfection. In (*C, D, F, G*), each bar represents mean ± SD from three biological replicates (N = 3). ns $p > 0.05$, *$p < 0.05$,**$p < 0.01$, ***$p < 0.001$. ****$p < 0.0001$. *p*-values were in (*C* and *D*) were calculated by two-way ANOVA followed by Tukey's multiple comparisons test, in F using unpaired two-tailed *t* test, and in G using one-way ANOVA followed by Dunnett's test. DOX, doxycycline; MTT, 3-(4,5-dimethylthiazol-2-yl)-2,5-diphenyltetrazolium bromide; RT-qPCR, reverse transcription quantitative PCR.

was the seventh-most correlated gene with SOX9 in terms of essentiality (Fig. S1*F*). In conjunction with our experimental data, these analyses strongly indicated that Wnt signaling and SOX9 working together was a general feature of CRC.

Since both Wnt signaling and SOX9 are major regulators of transcription, we wondered whether SOX9 could cooperate with the Wnt/β-catenin pathway to activate a common transcriptional program in CRC. One of the best-characterized Wnt targets in the context of CRC is the *MYC* oncogene (48), which is regulated by several WREs associated with CRC risk (33). In DLD-1 cells, *MYC* transcripts were downregulated by the combination of SOX9 knockdown and Wnt inhibition by dnTCF (Fig. 1*G*).

SOX9 directly binds and regulates the CRC risk-associated c-myc-335 WRE

After finding that *MYC* transcript levels were upregulated by Wnt signaling and SOX9, we wanted to study the regulatory interactions that allowed SOX9 to activate this Wnt target. One of the best-characterized WREs regulating *MYC* is the c-*myc*-335 enhancer containing a SNP (rs6983267) that increases CRC risk in humans and is regulated by TCF activity (11, 49, 50). Examination of a previously published SOX9 chromatin immunoprecipitation sequencing (ChIP-seq) dataset (51) showed that c-*myc*-335 was bound by SOX9 in HT-29 CRC cells (Fig. 2*A*). We verified this result in LS174T cells by performing ChIP using antibodies against β-catenin and
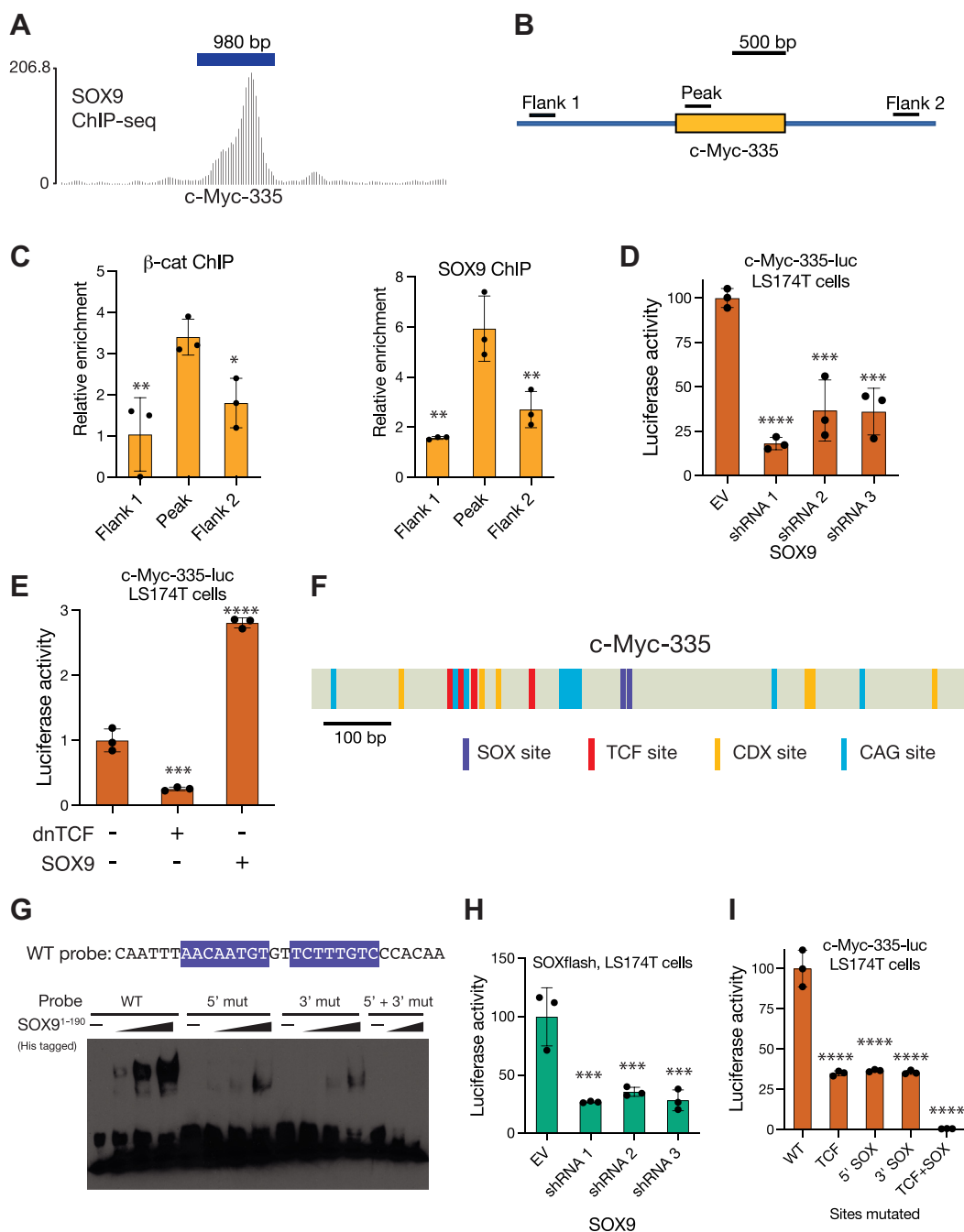
Figure 2. The colorectal cancer risk associated c-myc-335 WRE requires the direct binding of TCFs and SOX9 for its activation. *A*, ChIP-seq tracks showing the binding of SOX9 to the c-*myc*-335 locus in HT29 colorectal cancer cells. Dataset from (51). *B*, cartoon showing positions of primers used for ChIP-qPCR analysis of the c-*myc*-335 locus in LS174T colorectal cancer cells. *C*, ChIP-qPCR showing β-catenin, and SOX9 are enriched at the c-*myc*-335 locus in LS174T cells. ChIP signals were quantified by qPCR using primers shown in (*B*). *D*, RNAi against SOX9 reduces c-*myc*-335 reporter activity in LS174T cells. Cells were transfected with the reporter plasmid and plasmids encoding shRNAs against SOX9 or an empty vector (pSUPER). Luciferase activity was assayed 48 h post transfection. *E*, luciferase assay showing the effect of dnTCF and SOX9 overexpression on c-*myc*-335 reporter activity in LS174T cells. Cells were transfected with the reporter and plasmids encoding dnTCF, Flag-SOX9, or an empty vector (pcDNA3.1). Luciferase activity was assayed 24 h post transfection. *F*, cartoon of the c-*myc*-335 enhancer showing positions of the newly identified SOX-binding sites (*purple*) along with previously characterized TCF, CDX, and CAG sites (11). *G*, EMSA showing a recombinant SOX9 fragment containing the DNA-binding domain specifically binds to the newly identified binding sites on c-*myc*-335, and mutations in these sites abolish SOX9 binding. *H*, luciferase assay showing the effect of SOX9 RNAi on the activity of a synthetic reporter containing three tandem copies of the SOX9-binding sites from c-*myc*-335. Reporter was measured similarly as in (*D*). *I*, luciferase assay showing the effect of TCF and SOX site mutations on c-*myc*-335 reporter activity. WT and mutant reporters were transfected into LS174T cells and luciferase activity was assayed 24 h post transfection. In (*C–E, H, I*), each bar represents mean ± SD from three biological replicates (N = 3). ns $p > 0.05$, *$p < 0.05$,**$p < 0.01$, ***$p < 0.001$. ****$p < 0.0001$. *p*-values were calculated using one-way ANOVA followed by Dunnett's test. ChIP, chromatin immunoprecipitation; EMSA, electrophoretic mobility shift assay; qPCR, quantitative PCR; RT-qPCR, reverse transcription quantitative PCR.

SOX9. To detect ChIP enrichment, we compared quantitative PCR (qPCR) signals from primers located inside the enhancer to those from two primer sets flanking the enhancer (Fig. 2*B*) and found that β-catenin and SOX9 were both enriched at the enhancer (Fig. 2*C*).

Previous work from our group had generated a luciferase reporter driven by c-*myc*-335, which showed Wnt-dependent activity (11). In LS174T cells, we found that RNAi-mediated SOX9 depletion reduced c-*myc*-335 reporter activity (Fig. 2*D*). Wnt/β-catenin pathway inhibition with dnTCF repressed, while SOX9 overexpression activated the c-*myc*-335 reporter (Fig. 2*E*). In combination with the ChIP data, these results were consistent with a model of SOX9 directly binding and activating this enhancer in conjunction with TCFs and β-catenin.

To understand how SOX9 was recruited to this enhancer, we searched its sequence for potential SOX9-binding sites. Our previous work on the *cis*-regulatory logic of c-*myc*-335 had identified four TCF-binding sites, two sites bound by CDX proteins, and five repeated motifs, we named CAG sites, all of which contributed to enhancer activity (11). Using SOX9-binding site data from the JASPAR database, we scanned the c-*myc*-335 sequence for putative clusters of SOX9-binding sites. This search identified a pair of putative SOX-binding sites located adjacently in an inverted repeat orientation (Figs. 2*F* and S1*A*). The ability of SOX9 to dimerize and bind DNA is an important part of its ability to activate some of its transcriptional targets (52), and the binding sites in c-*myc*-335 were in the correct orientation to be bound by a SOX9 dimer. We confirmed the ability of SOX9 to bind to these predicted sites using a gel-shift assay. A purified His-tagged recombinant SOX9 fragment containing the DNA-binding domain (SOX9$^{1-190}$) induced a robust gel shift in a probe containing the WT SOX-binding sites and mutating either or both SOX9-binding sites in the probe attenuated the gel shift (Figs. 2*G* and S2*B*).

To functionally verify these SOX9-binding sites, we created a synthetic reporter containing multimerized copies of the SOX-binding sites upstream of a minimal promoter. The activity of this reporter, named "SOXflash," was SOX9 dependent, with reduced activity in LS174T cells upon RNAi-mediated SOX9 depletion (Fig. 2*H*). We then tested the contribution of SOX sites for WRE activation by mutating them in the c-*myc*-335-luc reporter. Previously, we found that mutating the four TCF sites caused a reduction in enhancer activity (11). Mutating either one of the SOX sites caused a reduction in enhancer activity comparable to mutating the four TCF-binding sites. Combined mutation of the TCF and SOX sites caused a nearly 200-fold reduction in enhancer activity (Fig. 2*I*). BLAST searches of the mouse and rat genomes showed that *MYC* enhancer regions in both species corresponding to human c-*myc*-335 also contained TCF- and SOX9-binding sites (Fig. S2*C*). Strikingly, the sequences of three out of the four TCF sites and one of the SOX9-binding sites are identical in humans, mice, and rats, suggesting that this mode of regulation is conserved among mammals.

SOX9 is important for activating a subset of WREs in cancer cells

Our analysis of the c-*myc*-335 WRE revealed that it was occupied by both TCFs and SOX9 and that its activity was dependent on both TCF- and SOX9-binding sites. While the c-*myc*-335 WRE is well known for its role in CRC risk, the *MYC* gene is surrounded by several WREs implicated in the misregulation of *MYC* in many different kinds of cancer (33). Our examination of HT-29 SOX9 ChIP-seq data (51) identified multiple putative SOX9-bound enhancers around the *MYC* locus (Fig. 3*A*). Comparing these regions with previously characterized WREs of *MYC*, we identified three WREs that overlap with SOX9-bound regions (Figs. 3*A*, S3–S5 and S6*A*) (33, 53–55). Analogous to c-*myc*-335, we named these regions Myc+8, Myc-29, and Myc-521, based on the distance in kilobases between the enhancers and the transcription start site of the *MYC* gene.

To confirm that these enhancers were jointly regulated by Wnt signaling and SOX9, we generated luciferase reporters by cloning these regions upstream of a minimal promoter and a luciferase coding sequence. In LS174T cells, both Myc+8 and Myc-29 were activated by SOX9 overexpression, which was silenced by the overexpression of the Wnt/β-catenin target repressor dnTCF (Fig. 3, *B* and *C*). We then tested Myc-521 in HepG2 hepatocellular carcinoma cells, which express a truncated form of β-catenin resulting in elevated Wnt signaling (56). Like Myc+8 and Myc-29, Myc-521 enhancer activity was stimulated by SOX9 overexpression and inhibited by additional dnTCF overexpression (Fig. 3*D*). These results suggest that SOX9 is a cofactor important for the activation of multiple *MYC* WREs in cancer cells.

Our findings raised the question of whether the positive role of SOX9 in WRE regulation was confined to *MYC* or whether other Wnt target genes in CRC were also activated by SOX9. We examined SOX9-bound regions in the HT-29 SOX9 ChIP-seq dataset (51) around Wnt-regulated genes from a HT-29 cell RNA-seq dataset (57). Of the top 5 high-confidence Wnt targets identified by this study, three genes (*NOTUM*, *SP5*, and *LARGE2*) had significant SOX9 peaks near their promoters and gene bodies, while no significant enrichment was seen near the other two (*NKD1, TGFB3*) (Fig. S6*B*). These findings suggest that SOX9 binds and regulates a subset of WREs in CRC cells.

Synergistic activation of Paneth cell markers by Wnt signaling and SOX9

To identify WREs regulated by Wnt signaling and SOX9 in the context of normal development, we examined genes expressed specifically in Paneth cells, which require both Wnt signaling and SOX9 for their differentiation (24, 27, 28). Transcript levels of two human Paneth cell marker genes, *Defensin alpha 5* (*Defa5*) and *Defensin alpha 6* (*Defa6*), have been recently shown to be upregulated in CRC cells by SOX9 overexpression (29). The promoters of two human Paneth cell markers, *Defensin alpha 5* (*Defa5*) and *Defensin alpha 6* (*Defa6*), are known to contain multiple TCF-binding sites, and
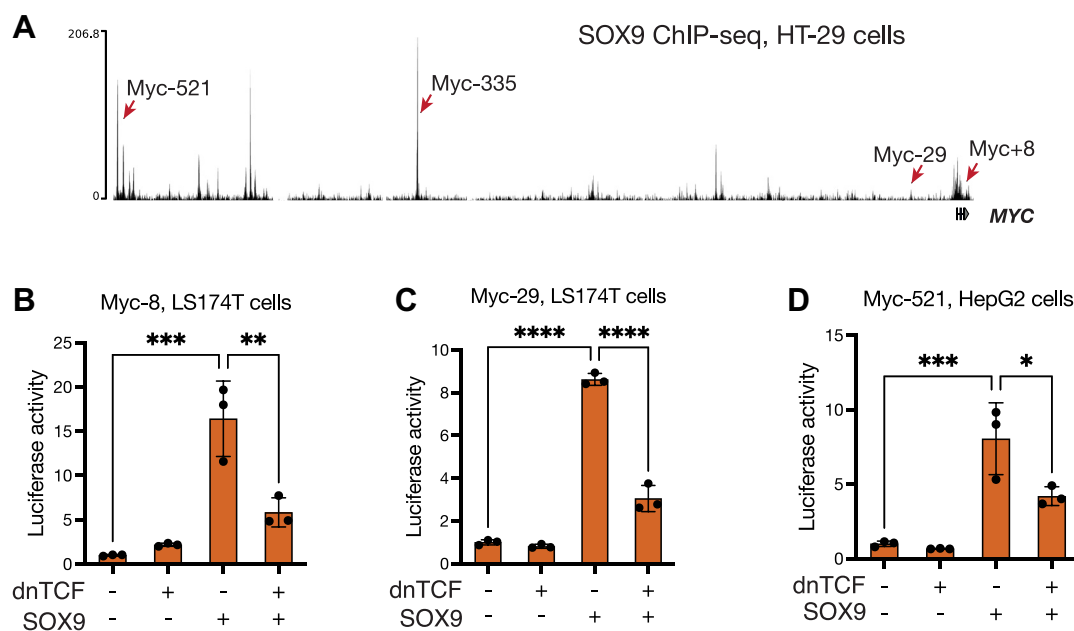
Figure 3. SOX9 and Wnt together regulate a multitude of WREs in cancer cells. *A*, SOX9 ChIP-seq tracks showing the *MYC* gene locus and the positions of cancer risk-associated WREs bound by SOX9 in HT29 cells. Dataset generated by (51). *B–D*, luciferase assays showing the effect of overexpressing dnTCF, SOX9, or both on the activity of the Myc+8, Myc-29, and Myc-521 reporters. Indicated cell lines were transfected with reporters and protein expression constructs 24 h before being assayed for luciferase activity. Each bar represents mean ± SD from three biological replicates (N = 3). ns $p > 0.05$, *$p < 0.05$,**$p < 0.01$, ***$p < 0.001$. ****$p < 0.0001$. *p*-values were calculated using one-way ANOVA followed by Dunnett's test. ChIP-seq, chromatin immunoprecipitation sequencing; WRE, Wnt-regulated element.

transcriptional reporters made from these promoters are activated by Wnt signaling in cell culture (30, 31). We were interested in whether these Paneth cell WREs were also directly regulated by TCFs and SOX9.

To test whether *Defa5* was coregulated by SOX9 and the Wnt/β-catenin pathway, we examined its expression in a HEK293 cell line with a DOX-inducible SOX9 overexpression construct (DOX-SOX9 cells) (22). We found that *Defa5* mRNA levels were synergistically upregulated under high-Wnt and high-SOX9 levels induced by DOX treatment in conjunction with the β-catenin destruction complex inhibitor CHIR-99021 (Fig. 4*A*). There was no detectable *Defa6* mRNA expression in these cells. We then cloned the promoters of both *Defa5* and *Defa6* into the pGL4.10 promoterless luciferase reporter plasmid to generate transcriptional reporters for both genes (referred to as Defa5-luc and Defa6-luc). We tested the response of both reporters to SOX9 overexpression and Wnt/β-catenin pathway stimulation by the overexpression of a stabilized β-catenin (containing the S33Y mutation, referred to as β-catenin*) (58). Defa5-luc was not significantly activated by β-catenin* or SOX9 overexpression individually but showed synergistic activation in the presence of both (Fig. 4*B*). Defa6-luc was activated by SOX9 overexpression but showed maximal activity under high-Wnt and high-SOX9 conditions similar to those found in Paneth cells (Fig. 4*C*). In LS174T cells, which already have high levels of Wnt signaling, SOX9 overexpression activated Defa5 and Defa6 promoter activity, which was repressed by inhibiting Wnt signaling with dnTCF (Fig. 4, *D* and *E*).

We then probed the *cis*-regulatory logic of the *Defa5/6* promoters. Computational searches for TF-binding sites identified putative TCF- and SOX-binding sites in the

promoters of *Defa5/6*, in addition to the CDX and CAG sites identified in several other WREs (Figs. 4*F*, S7, *A* and *B*). We tested the importance of these sites by mutating the TCF, SOX, CDX, and CAG sites in *Defa5* and the TCF and SOX sites in *Defa6*. Measurements of reporter activity in HEK293T cells under high Wnt and high SOX9 conditions (Fig. 4, *G* and *H*) and in LS174T cells with SOX9 overexpression (Fig. S7, *C* and *D*) showed that all four sets of motifs were essential for WRE activity. Put together, these results indicate that in addition to working together to direct Paneth cell fate, Wnt signaling and SOX9 continue to be important after differentiation by directly activating genes expressed in Paneth cells using a regulatory logic similar to that seen in SOX9-activated oncogenic enhancers of *MYC*.

TCF- and SOX-binding sites are sufficient for synergistic enhancer activation by Wnt signaling and SOX9

While we found no evidence of SOX9 repressing the Wnt/β-catenin pathway in LS174T and DLD-1 cells, SOX9 is known to potently repress WRE expression in HEK293T cells (22), making the identification of WREs that were activated synergistically by Wnt signaling and SOX9 in HEK293T cells very striking. Previous work from our group characterized CREAX, a distal Wnt-responsive enhancer of the *Axin2* Wnt target gene and found that enhancer activity was mediated by a combination of TCF, CDX, and CAG sites (11). However, CREAX lacks SOX9-binding sites and is repressed by SOX9 overexpression (22). While the Defa5/6 and c-*myc*-335 WREs also contain TCF, CDX, and CAG sites, they were set apart from CREAX by the presence of SOX9-binding sites. This
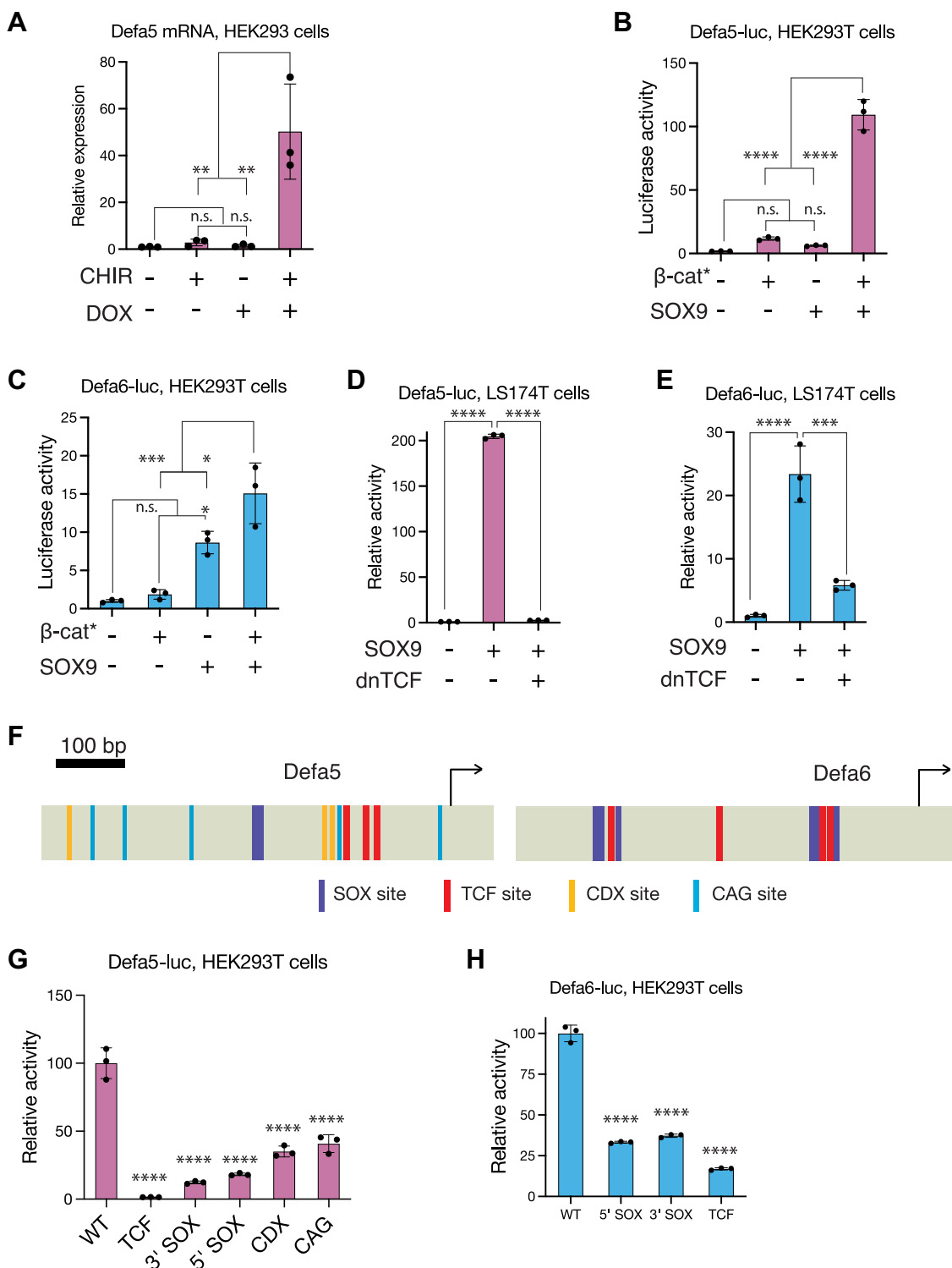
Figure 4. SOX9 and Wnt signaling synergistically drive Paneth cell defensin activity through TCF and SOX binding sites. *A*, RT-qPCR data showing induction of *Defa5* mRNA levels under high Wnt, high SOX9 levels. DOX-SOX9 HEK293 cells (22) were treated with CHIR-99021 to activate Wnt signaling and DOX to activate SOX9 overexpression. Transcript levels were measured 24 h after treatment. *B*, induction of Defa5-luc reporter activity by Wnt signaling and SOX9 in HEK293T cells. *C*, induction of Defa6-luc reporter activity by Wnt signaling and SOX9 in HEK293T cells. *D*, activation of Defa5-luc reporter activity by SOX9 overexpression and repression by dnTCF overexpression in LS174T cells. *E*, activation of Defa6-luc reporter activity by SOX9 overexpression and repression by dnTCF overexpression in LS174T cells. *F*, cartoons of the promoters of *Defa5* and *Defa6* showing the locations of TCF, SOX, CDX, and CAG sites. *G*, loss of Defa5-luc reporter activity upon mutation of TCF, SOX, CDX, or CAG sites. *H*, loss of Defa6-luc reporter activity upon mutation of TCF or SOX sites. For (*B–E*, *G*, and *H*), cells were transfected with indicated reporters and plasmids expressing stabilized β-catenin (β-catenin*), Flag-SOX9, dnTCF, or empty vector (pcDNA3.1). Luciferase activity was measured 24 h post transfection. Each bar in (*A–E*, *G*, *H*) represents mean ± SD from three biological replicates (N = 3). ns $p > 0.05$, *$p < 0.05$, **$p < 0.01$, ***$p < 0.001$. ****$p < 0.0001$. *p*-values in (*A–C*) were calculated by one-way ANOVA followed by Tukey's test, and in (*D*, *E*, *G*, *H*) using one-way ANOVA followed by Dunnett's test. DOX, doxycycline; RT-qPCR, reverse transcription quantitative PCR.

suggested that the *cis*-regulatory grammar of these WREs was the sole determinant of whether they were activated or repressed by SOX9.

To directly test this idea, we generated a synthetic enhancer with a combination of TCF- or SOX9-binding sites. Reporters containing only multimerized TCF-binding sites (TOPflash) are robustly activated by Wnt signaling (59), and similar reporters containing SOX9-binding sites (SOXflash) show SOX9-dependent enhancer activity (Fig. 2*H*). Our new

reporter, named TOP/SOX, contains two TCF and two pairs of SOX9-binding sites in the dimer-binding orientation (Figs. 5*A* and S8). In LS174T cells, TOP/SOX-luc was repressed by dnTCF and activated by SOX9 overexpression, mimicking the expression pattern of the c-*myc*-335 enhancer (compare Figs. 5*B* and 2*E*).

We then compared the response of TOPflash, SOXflash, and TOP/SOX in HEK293T and HeLa cells to the overexpression of β-catenin*, SOX9, or both. As expected,
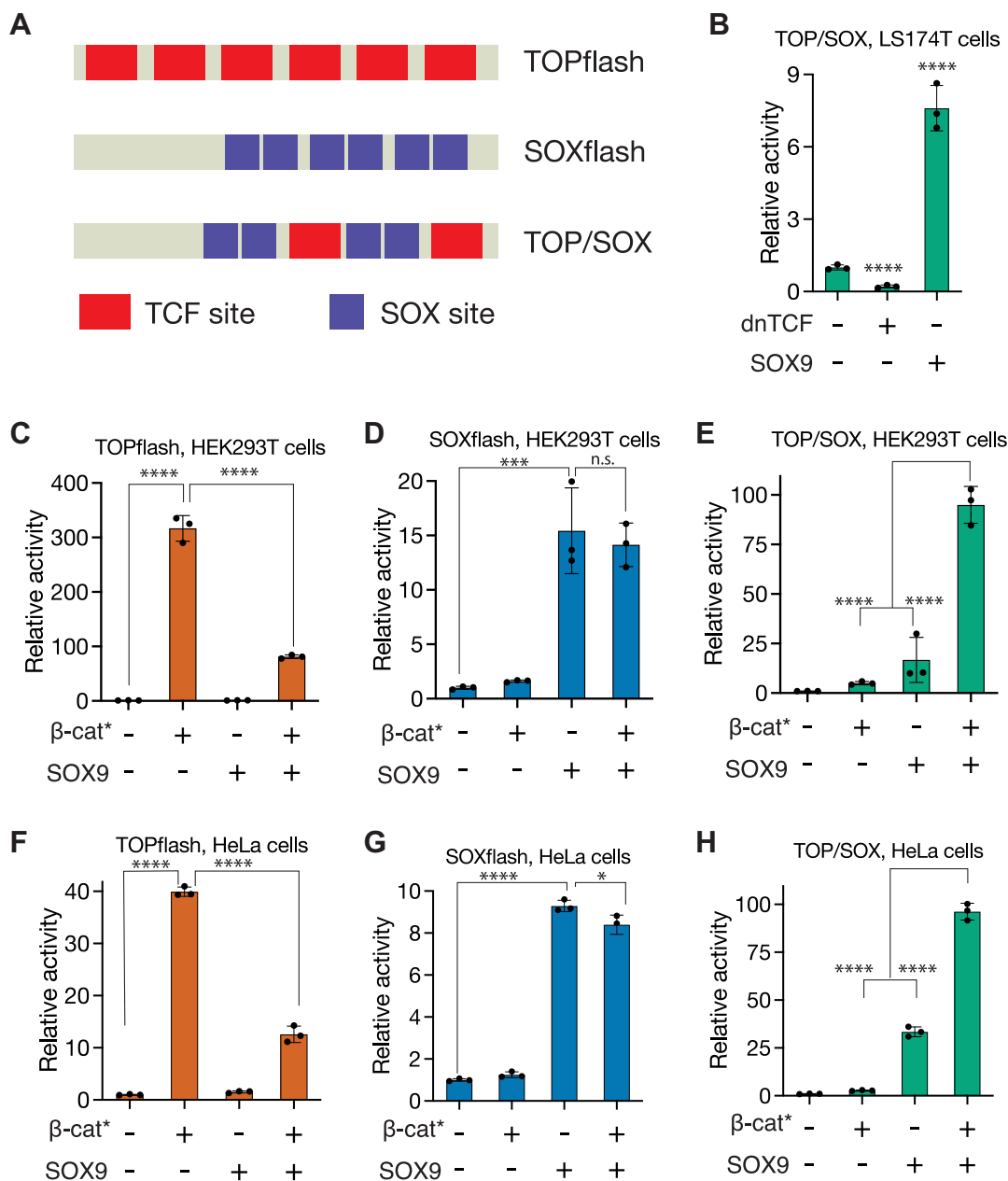

Figure 5. TCF and SOX binding sites are sufficient for synergistic enhancer activation by Wnt signaling and SOX9. *A*, cartoons of synthetic enhancers containing combinations of TCF and SOX binding sites. TOPflash contains only TCF sites, SOXflash contains only SOX sites, and TOP/SOX contains both TCF and SOX sites. *B*, TOP/SOX is repressed by dnTCF overexpression and activated by SOX9 overexpression in LS174T cells. *C–H*, relative activity levels of TOPflash, SOXflash, and TOP/SOX in HEK293T (*C–E*), and HeLa cells (*F–H*) upon stimulation of Wnt signaling, SOX9 overexpression, or both. Cells were transfected with indicated reporters and overexpression constructs, and luciferase activity was assayed 24 h later. Each bar represents mean ± SD from three biological replicates (N = 3). ns $p > 0.05$, *$p < 0.05$,**$p < 0.01$, ***$p < 0.001$. ****$p < 0.0001$. *p*-values were calculated using one-way ANOVA followed by Dunnett's test.

TOPflash activity was robustly induced by β-catenin* and repressed by SOX9 overexpression (Fig. 5C). In contrast, SOXflash was robustly activated by SOX9 overexpression and not significantly affected by β-catenin* (Fig. 5D). Strikingly, TOP/SOX was maximally activated by the combined overexpression of both β-catenin* and SOX9 (Fig. 5E). A similar pattern of expression was seen in HeLa cells, with TOP/SOX showing a qualitatively different expression pattern to TOPflash and SOXflash (Fig. 5, F–H). The conditions that cause dramatic reductions in TOPflash activity are identical to those that result in maximal activation of TOP/SOX (Fig. 5, C and F). Our data demonstrate that within a single cell type, the presence or absence of SOX9-binding sites can determine whether a WRE is repressed or activated by SOX9.

TCFs and SOX9 directly interact through non-DNA contacting residues in their DNA-binding domains

Multiple SOX family members have been shown to complex with TCFs through their DNA-binding HMG domains (12), and we wondered if the same was true in the case of SOX9. We tested the ability of purified recombinant glutathione-*S*-transferase (GST)-tagged LEF1 and TCF7 to interact with His-tagged SOX9 in a pull-down assay, with GST as a negative control. Full-length SOX9 directly bound to both LEF1 and TCF7 *in vitro* (Fig. 6, A and B). A GST-tagged fragment of LEF1 containing just the HMG domain (Fig. 6A) also robustly pulled down full-length SOX9 (Fig. 6C), suggesting that like other TCF-SOX protein interactions, TCF-SOX9 interactions were also mediated by HMG domains. To eliminate the possibility that this interaction was scaffolded by residual bacterial DNA in our purified protein preparations, we tested the impact of Mnase treatment and found no effect on the interaction between the HMG domains of LEF1 and SOX9 (Fig. S9A). This confirmed that the HMG domain of SOX9 could directly interact with the HMG domain of TCFs, independent of DNA binding.

To test the importance of TCF/SOX9 interactions in gene regulation, we wanted to generate a separation-of-function mutant of SOX9 that retained its ability to bind to DNA but could not bind to TCFs. An analysis of a crystal structure of the HMG domain of SOX9 complexed with DNA (Protein Data Bank ID: 4EUW) revealed the presence of multiple charged residues on the outer surface of the HMG domain. Working off the hypothesis that the TCF/SOX9 interaction was mediated by charged residues whose side chains pointed away from the DNA, we tested constructs containing charge swap mutations for their ability to bind to the HMG domain of LEF1. We found that a SOX9 HMG domain fragment containing mutations changing three aspartate (acidic) residues in SOX9 (D125, D168, and D171) to lysines (basic) showed no detectable binding to the HMG domain of LEF1 (Fig. 6, D and E). These results suggested that TCFs and SOX9 bound to each other through salt bridges mediated by non-DNA contacting residues on their HMG domains. They also provided us with a reagent that could be used to test the role of TCF/SOX9 protein–protein interactions in gene regulation. The
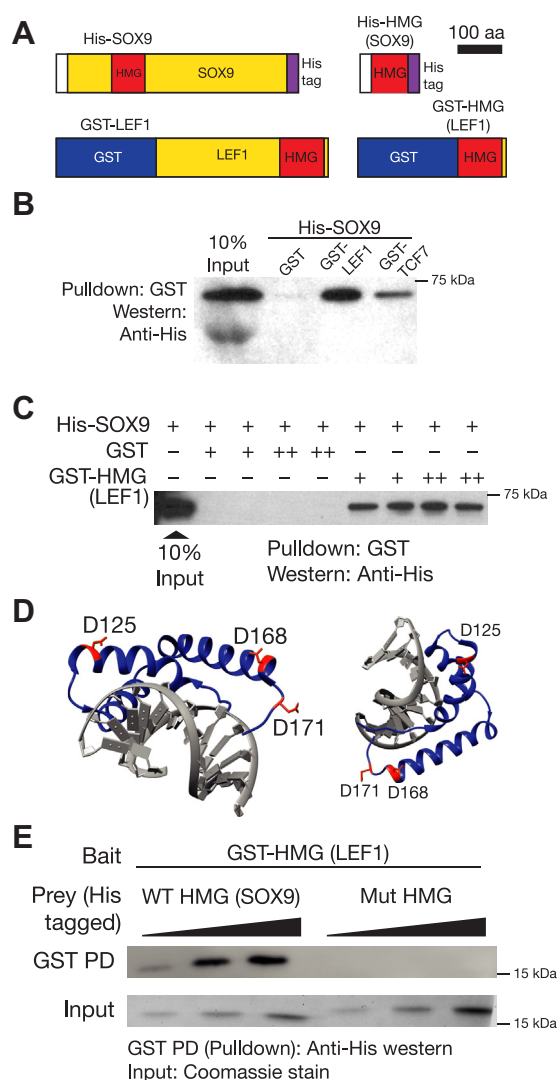

Figure 6. SOX9 directly binds to TCFs through non-DNA contacting residues in its DNA-binding HMG domain. *A*, cartoons of GST-tagged LEF1 and His-tagged SOX9 fragments used for pull-down experiments. *B*, GST pull down showing direct binding of SOX9 to LEF1 and TCF7. *C*, GST pull down showing binding of full-length SOX9 to the HMG domain of LEF1. *D*, two views of a crystal structure of the SOX9 HMG domain (PDB ID: 4EUW). Amino acid residues mutated to abolish TCF binding are colored *red* with their side chains shown. *E*, mutation of three amino acids in SOX9's HMG domain (D125, D168, and D171) abolishes the TCF-SOX interaction. Purified His-tagged proteins were pulled down using glutathione beads with indicated GST-tagged proteins as bait for (*B*, *C*, and *E*). GST was used as negative control. PDB, Protein Data Bank.

interacting residues were highly conserved across vertebrate orthologs of SOX9 (Fig. S9B), suggesting that TCF-SOX9 interactions may be important for gene regulation across many species. Within human SOX proteins, the three residues were highly conserved (identical or conserved mutation) in the SOXE (SOX8,9,10) and SOXC (SOX4,11,12) subfamilies, with limited conservation in other family members (Fig. S10). We examined the correlation between the conservation of these residues and the ability of SOX proteins to suppress or synergistically activate targets in a Wnt/β-catenin dependent manner. Only one of the residues is conserved in SOX2 and SOX7, while none of them are conserved in SRY (Fig. S11A). When overexpressed in HEK293T cells, SOX9, SOX2, SRY,

and SOX7 could all suppress β-catenin*-driven TOPflash reporter activity (Fig. S11, *B* and *C*). However, only SOX9 was able to synergistically activate the Defa5-luc reporter along with β-catenin* (Fig. S11*D*).

TCF/SOX9 interactions are essential for synergistic enhancer activation and cancer cell survival

Before using our novel mutant to test the importance of TCF/SOX9 interactions for gene regulation, we wanted to ensure that the mutations did not compromise the ability of SOX9 to perform its TCF-independent functions. First, we compared the ability of WT and D125,168,171K mutant (Mut) SOX9 to activate the SOXflash reporter in HEK293T cells.

Transfection of identical amounts of plasmid expressing WT or Mut SOX9 produced similar activation of SOXflash (Fig. 7*A*). The ability of SOX9 to repress Wnt reporters such as TOPflash involves the transcriptional activation of the SOX9 target gene MAML2 (22). In HEK293T cells, both WT and mutant suppressed β-catenin*-induced TOPflash activation to similar levels (Fig. 7*B*). These experiments suggested that the ability of SOX9 to enter the nucleus, complex with DNA, and mediate transcriptional activation was not affected by the HMG domain mutations.

We then compared the ability of WT and Mut SOX9 to drive c-*myc*-335 enhancer activity. While the overexpression of WT SOX9 could rescue the loss of reporter activity caused by SOX9 RNAi, overexpression of Mut SOX9 at similar levels
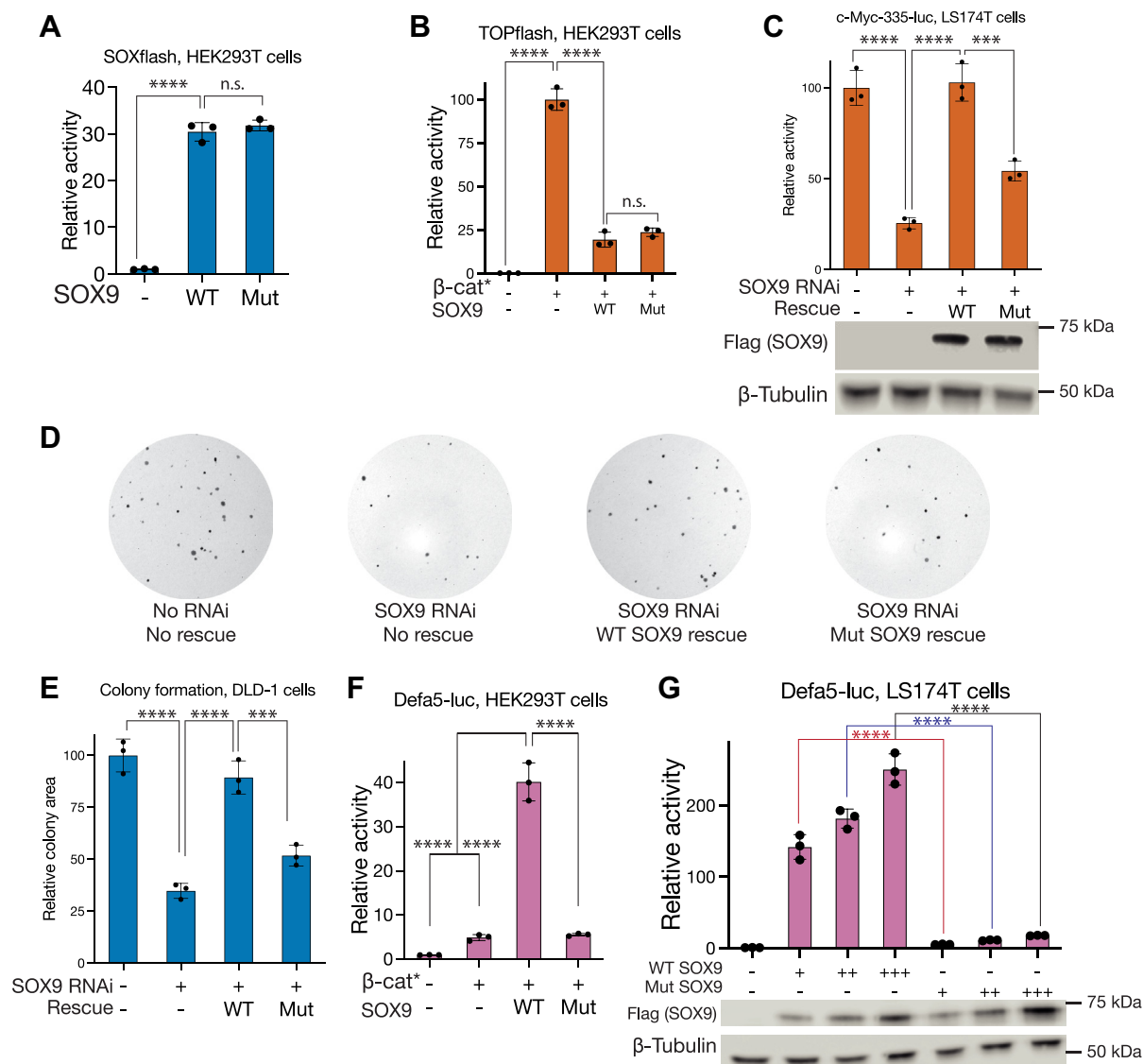

Figure 7. TCF/SOX interactions are essential for WRE activity and colorectal cancer cell growth. *A*, luciferase assay showing that SOXflash activity can be driven by both WT and TCF interaction-deficient (Mut) SOX9. *B*, luciferase assay showing both WT and Mut SOX9 are equally capable of suppressing TOPflash activation by β-catenin*. *C*, luciferase assay showing that WT SOX9 but not Mut can rescue the loss of c-*myc*-335 reporter activity caused by SOX9 RNAi in LS174T cells. Western blots show relative expression levels of WT and Mut SOX9. *D*, representative images showing that WT SOX9 but not Mut can rescue the loss of colony formation caused by SOX9 RNAi in DLD-1 cells. *E*, quantification of the area occupied by colonies in (*D*). *F* and *G*, luciferase assays showing that Defa5-luc can be activated by WT but not Mut SOX9 in HEK293T and LS174T cells. Western blots in (*G*) show relative expression levels of WT and Mut SOX9. Each bar represents mean ± SD from three biological replicates (N = 3). ns *p* > 0.05, **p* < 0.05,***p* < 0.01, ****p* < 0.001. *****p* < 0.0001. *p*-values were calculated using one-way ANOVA followed by Dunnett's test for (*A*) and Tukey's test for all other panels. WRE, Wnt-regulated element.

only resulted in a partial rescue (Fig. 7C). Similarly, over-expression of WT but not Mut SOX9 rescued the colony formation defect in DLD-1 cells caused by SOX9 RNAi (Fig. 7, D and E). In the case of Defa5-luc, the overexpression of Mut SOX9 along with β-catenin* failed to produce the synergistic activation shown by WT SOX9 in HEK293T cells (Fig. 7F). In LS174T cells, overexpression of Mut SOX9 produced a very attenuated activation of the Defa5-luc reporter when compared to similar levels of WT SOX9 overexpression (Fig. 7G). Finally, Mut SOX9 also showed a compromised ability to activate the Defa6-luc reporter in concert with β-catenin* in HEK293T cells (Fig. S12A), and its over-expression in LS174T cells resulted in reduced Defa6-luc re-porter activation when compared to WT SOX9 (Fig. S12B). Put together, these results suggest that a combination of *cis*-regulatory grammar and TCF/SOX9 protein–protein in-teractions is essential for activating a Wnt/SOX9 target gene program that allows Paneth cell gene expression and the growth and survival of CRC cells.

Discussion

How the interplay between signaling-dependent develop-mental regulators like the Wnt/β-catenin pathway and lineage-determining transcription factors such as SOX proteins results in spatiotemporally diverse patterns of gene expression is a fundamental question in developmental biology. Prior to this study, models of SOX9's role in Wnt signaling characterized SOX9 as a Wnt/β-catenin pathway repressor, primarily influ-enced by work on the mammalian sex determination pathway and cell culture studies that examined the effects of SOX9 overexpression on Wnt signaling (12). In conjunction with several recent studies (29, 39, 40), our findings demonstrate a highly context-specific role for SOX9 in CRC, in which it promotes the growth and survival of CRC cells (Fig. 1). This transcriptional program involves SOX9 directly binding and regulating a subset of WREs (Figs. 2 and 3). Findings of SOX9 activating Paneth cell markers suggest a role for Wnt signaling and SOX9 cooperating to activate gene expression during both normal and cancerous growth (Fig. 4). Whether SOX9 acti-vates or represses a given WRE is determined by the presence or absence of SOX9-binding sites (Fig. 5), and the ability of SOX9 to complex with TCFs is integral to its ability to activate Wnt targets (Figs. 6 and 7). In addition to the well-characterized binding between β-catenin and TCFs (60), SOX9 and β-catenin have also been reported to interact in coimmunoprecipitation and protein–protein binding assays (20, 61). While our data do not directly address whether these proteins form a trimeric complex, it is worth noting that the β-catenin–binding site on TCFs is at the N terminus (60), distinct from the HMG domain that we found is sufficient for binding SOX9 (Fig. 6, C and E). Further study is needed to elucidate the biochemical relationship between TCFs, SOX9, and β-catenin on chromatin when they activate specific Wnt targets.

Previous work on SOX9 identified a naturally occurring shorter isoform of SOX9, named miniSOX9, that was expressed in many CRC lines (61). When overexpressed, miniSOX9 inhibited SOX9-driven reporter activity and also alleviated SOX9's inhibition of Wnt readouts, leading to a model of miniSOX9 as a naturally occurring dominant nega-tive variant that allowed the *SOX9* gene to stimulate cancer growth by inhibiting the ability of full-length SOX9 to repress Wnt signaling (61). However, this model was not tested directly with loss-of-function experiments. Our data show that SOX9 does not repress the Wnt/β-catenin pathway in CRC cells at endogenous levels of expression (Figs. 1A and S1A). Additionally, overexpression of full-length SOX9 was sufficient to rescue the loss of colony formation after SOX9 KD (Fig. 7, D and E) targeting the 5′-UTR that is shared by full-length and WT SOX9 (61). These results establish a role for the full-length SOX9 protein in promoting cancer growth by tran-scriptional activation.

Our examination of the regulatory logic of SOX9-activated WREs revealed the presence of functionally important TCF- and SOX9-binding sites without any easily discernible binding site grammar (Figs. 2 and 4). While the validated TCF- and SOX-binding sites in c-*myc*-335 and the *Defa5* promoter are separated by several dozen nucleotides, they are more tightly clustered in the *Defa6* promoter (Figs. 2F and 4F). Similarly, the predicted TCF- and SOX9-binding sites in Myc+8, Myc-29, and Myc-521 also do not follow a readily observable pattern of binding site grammar. Alignments of the four en-hancers of *MYC* across humans, mice, and rats indicate that while some of the predicted TCF- and SOX9-binding sites are phylogenetically conserved, each species also has unique and nonconserved predicted TCF/SOX9-binding sites (Figs. S2– S5). This supports the view that there is little constraint on the positioning of these sites. A similar comparison was not possible for *Defa5/6* due to the high species-specific evolu-tionary divergence of the *Defensin* gene family (62). Together with our synthetic reporter experiments (Fig. 5), this suggests that the mere presence or absence of SOX-binding sites is sufficient to discriminate between activation and repression of WREs by SOX9. While some of the SOX9-binding sites characterized in this study are in the correct orientation to be bound by SOX9 dimers, others are singular binding sites. Previous work has shown that the ability of SOX9 to dimerize is crucial for its role in some contexts such as chondrogenesis, but not in others such as the mammalian sex determination pathway (52, 63). In this study, we only tested the effect of individual SOX-binding site mutations in the context of c-*myc*-335 and *Defa5*, which have a single pair of SOX9-binding sites each. While these data might indicate a role for SOX9 dimerization in Wnt target gene regulation, more mutagenesis experiments and experiments using dimerization-deficient mutants are required to test it directly.

Previous work has shown that when overexpressed, SOX9 inhibits WREs in a dose-dependent manner. SOX9 over-expression results in the transcriptional upregulation of *MAML2*, which promotes β-catenin degradation (22). At the same time, overexpression of SOX9 in CRC cells with high levels of Wnt signaling activates a Paneth cell–like gene expression program (29). While intestinal stem cells retain

their ability to proliferate and differentiate in the absence of SOX9 (27, 28), they do show changes in their gene expression patterns after SOX9 removal (64). The requirement of SOX9 for proliferation in these cell types has led to the idea that a "critical dose" of SOX9 may be important for intestinal stem and cancer cell proliferation (38, 65). Our findings support this model and provide a molecular basis for it. The ability of SOX9 to promote the expression of a subset of Wnt target genes makes it an essential regulator of growth and proliferation in these cells. Genes coregulated by Wnt signaling and SOX9 may also show differential sensitivity to SOX9 levels. For example, the c-*myc*-335 enhancer showed high activity at the endogenous SOX9 levels seen in LS174T CRC cells and was only modestly activated by SOX9 overexpression (Fig. 2*E*). In contrast, the promoters of *Defa5/6*, which are active in Paneth cells that express higher levels of SOX9, were significantly activated by SOX9 overexpression (Fig. 4*D*). Our finding that Wnt/SOX9-activated enhancers are most active under conditions that lead to a partial inhibition of WREs lacking SOX9-binding sites (Fig. 5) may provide a mechanistic explanation for the "critical dose" model, with higher levels of SOX9 shutting down WRE activity through β-catenin degradation, and lower levels of SOX9 preventing the activation of some WREs, leading to reduced proliferation under both reduced and increased SOX9 levels.

While hyperactivated Wnt signaling has long been known as a driver of CRC, its important role in driving the homeostasis of many different adult tissues has proved an important roadblock for the use of Wnt/β-catenin pathway inhibition as a cancer therapy (1, 32, 66–68). Our identification of the importance of SOX9-TCF interactions as a driving force for Wnt target gene activation in CRC may allow the development of novel therapeutics for CRC that disrupt the TCF-SOX9 interaction. Short peptides that mimic TF-TF interaction domains have been used in the past to successfully and specifically disrupt TF binding *in vivo* (69). Similar peptides may allow the specific inhibition of Wnt signaling in cancer cells without depleting the many Wnt-dependent stem cell populations found in the body.

Experimental procedures

Cell culture and transfection

Cell lines were grown at a temperature of 37 °C with 5% CO_2. HEK293T (ATCC, CRL-3216) and DLD-1 (ATCC, CCL-221) cells were grown in Dulbecco's modified Eagle's medium (Gibco, 11995065) supplemented with 10% fetal bovine serum (FBS) and penicillin/streptomycin/glutamine (Gibco, 10378016). HepG2 cells were a kind gift from Dr Jun Wu (University of Michigan). The LS174T-derived pTer-β-catenin-RNAi stable line (pTer-β-cat) was a kind gift from Dr Xi He (Boston Children's Hospital, Harvard Medical School. LS174T cells (ATCC, CL-188); their derivatives and HepG2 cells were grown in minimum essential medium (Gibco, 11095080) with 10% FBS and penicillin/streptomycin/glutamine. Tetracycline-screened FBS (Cytiva, SH30071.03T) was used to culture pTer-β-cat cells and their derivatives. pTer-β-

cat cell media was supplemented with 100 µg/ml Zeocin (InvivoGen, ant-zn-05) to select for the β-catenin RNAi cassette.

Lentiviral supernatants were produced at the University of Michigan Vector Core. To generate cells stably expressing nontargeting (scrambled) or SOX9-targeting shRNAs (details in Table S1), cells were incubated with viral supernatants overnight. Cells were thereafter maintained in 1 µg/ml puromycin to select for the Scrambled or SOX9 shRNA expressing cassette.

Transient transfections of HEK293T, HepG2, and LS174T cells were done with PEI MAX (Polysciences, 24765-1). DLD-1 cells were transfected with Lipofectamine 2000 (Invitrogen, 11668030) according to manufacturer's instructions.

Plasmids

SOX9 RNAi plasmids used to generate stable LS174T cell lines were from the pGIPZ library and purchased from the University of Michigan Vector Core (details in Table S1). shRNA constructs used for transient transfection experiments were cloned into the pSUPER vector (Oligoengine, VEC-pBS-0002) (details in Table S2). Empty pSUPER plasmid was used as negative control. The c-*myc*-335 locus was amplified *via* PCR using human Jurkat cell genomic DNA as a template and cloned into XhoI/BglII sites in pGL4.23 (Promega, E8411). dnTCF (70) and Flag-SOX9 (22) constructs have been described previously. TF-binding site mutations in c-*myc*-335 were generated using a combination of Gibson assembly and site-directed PCR mutagenesis. Details of mutations are specified in Table S3. Myc+8, Myc-29, and Myc-521 reporters were amplified from HEK293T cell genomic DNA and cloned into pGL4.23 between the XhoI and HindIII restriction sites. The sequence of the region between these sites is shown in Figs. S3–S5. Human β-catenin* containing the S33Y mutation was cloned into the pcDNA3.1 vector and was a gift from Dr Eric Fearon, University of Michigan. *Defa5/6* reporters were PCR amplified from human genomic DNA and cloned into the pGL4.10 promoterless luciferase vector (Promega, E6651) between the XhoI and KpnI restriction sites. gBlock fragments containing mutations in TF-binding sites were ordered from IDT and cloned into these plasmids to generate site mutant reporters. Details of mutations are specified in Table S4. Oligonucleotides containing fragments of the TOP/SOX reporter sequence were ordered from IDT, annealed together, and cloned into the pGL4.23 vector. The sequence of the synthetic reporter is shown in Fig. S8. GST-tagged TCF7 has been previously described (11). GST-tagged LEF1 was generated similarly by cloning the LEF1 ORF between the BamHI/NotI sites of pGEX-6p-1. His-tagged SOX9 was generated by cloning the ORF into the BamHI/SalI sites of pET-52b. HMG domain fragments of LEF1 and SOX9 were PCR amplified and cloned into pGEX-6p-1 and pET-52b between the same restriction sites used to make the full-length expression constructs. D125,168,171K mutations were introduced in the His-HMG and Flag-SOX9 expression plasmids using PCR with mismatched primers followed by Gibson assembly. To create a

Flag-SOX2 expression plasmid, the Flag-SOX9 expression plasmid was restriction digested with BamHI and XhoI. SOX2 complementary DNA was PCR amplified from a tagged SOX2 ORF clone (Origene, RC200757) using primers containing BamHI and XhoI sites. The PCR product was digested with the two enzymes and ligated into the vector. A sequence encoding the Flag-SRY construct was ordered as a gBlock from IDT and cloned between the BamHI/XhoI sites of pcDNA3.1. The SOX7 expression plasmid was a kind gift from Prof. Injune Kim, Graduate School of Medical Science and Engineering, Korea Advanced Institute of Science and Technology.

Colony formation assays

Cells were plated in 12-well plates and transfected or treated with DOX for the indicated amounts of time. Ultrapure water (solvent) was used as negative control for DOX experiments. Following this, they were resuspended in the appropriate cell culture media after treatment with 0.25% Trypsin-EDTA. Cell numbers were determined for each condition using a hemocytometer. Cells were then diluted to obtain the final concentrations reported in each experiment and then seeded in triplicates onto 6-well plates. They were allowed to grow undisturbed for 12 to 14 days until colonies were easily visible to the naked eye. Colonies were fixed with methanol for 20 min, following which they were stained with crystal violet staining solution (0.5% (w/v) crystal violet, 20% methanol) for 10 min. They were then rinsed with distilled water, dried overnight, and imaged.

The area occupied by the colonies was quantified using Fiji (71). Each well was defined as a circular region of interest and then cropped out. Wells were individually thresholded and the fraction of the area occupied by the wells was measured.

MTT assay for cell number

MTT assays were carried out using Cell Proliferation Kit I (Roche, 11465007001). Cells expressing scrambled or SOX9 shRNAs were plated onto 48-well plates with and without DOX at a density of 30,000 cells/well. Serial dilutions of cells were plated to determine a standard curve. Forty-eight hours later, 20 µl of MTT labeling reagent was added to each well. About 200 µl of solubilization solution was added 4 h later. Absorbance was measured at 565 nm using a Tecan Infinite 200 plate reader. Relative cell densities of the different samples and treatments were then calculated based on the standard curve. All measurements were done with biological triplicates.

Reverse transcription quantitative PCR for transcript quantification

RNA was extracted using the Rneasy mini kit (Qiagen, 74104). Reverse transcription was then performed using Superscript III Reverse Transcriptase (Invitrogen, 18080093). The Power SYBR Green PCR master mix (Applied Biosystems, 4368577) was used to perform PCRs using a CFX Connect Real-Time PCR Detection System (Bio-Rad, 1855201). Mean and SDs of transcript levels were quantified using the delta-delta Ct method using *G6PD* transcript levels for normalization. All measurements were done with biological triplicates. Primers are shown in Table S5.

ChIP

ChIP was performed and signals were quantified using qPCR as previously described (11). SOX9 ChIP was done using an anti-SOX9 antibody (Sigma, AB5535). For β-catenin ChIP, cells were first treated with the protein-protein crosslinker EGS (ethylene glycol bis(succinimidyl succinate)) (Thermo Scientific, 21565) at a concentration of 12.5 mM (70), following which ChIP was performed using an antibody targeting active β-catenin (CST, 8814S). One set of primers for qPCR (Table S6) was designed to amplify inside the c-*myc*-335 enhancer region and two primer pairs were designed to amplify flanking regions outside the enhancer for comparison. ChIP signals from each of these primers were compared to the signal from a control region to quantify enrichment. Primers used for ChIP are shown in Table S6.

ChIP-seq data analysis

ChIP-seq data analyzed in this study was generated by a previous study (51). Publicly available data were downloaded from GEO (accession number: GSE63629). The data file GSM1554224_HT29_SOX9_antibody.bar was converted into bedgraph format using USeq (72). ChIP-seq track visualizations were generated using pyGenomeTracks (73).

Computational analysis of TF-binding sites

TCF, CDX, and CAG sites were computationally annotated using FIMO (74) as previously described (11). Initial identification of SOX9-binding sites was based on the SOX9 MA0077.1 motif file from the JASPAR database (75). To ensure the identification of potential SOX9 dimeric binding sites, searches were repeated with lowered thresholds to look for lower scoring sites in the correct orientation located adjacent to high-scoring sites.

Luciferase assays and analysis

Luciferase assays were done with firefly luciferase reporter plasmids and constitutively expressed renilla luciferase as an internal transfection control. Luciferase activity was measured using Promega's Dual Luciferase Assay system (Promega, E1910) according to manufacturer's protocols. Firefly/renilla ratio was used as the measure of activity for each well. All assays were done in triplicates, following which the mean and SD of firefly/renilla ratios were calculated for each experimental condition. To calculate relative luciferase activity, a basal condition was selected (specified in each figure) and the ratios of all conditions were expressed in proportion to it.

Electrophoretic mobility shift assay

His-tagged SOX9$^{1-190}$ was expressed and purified as indicated later. Binding reactions were carried out in binding buffer (10 mM Tris-Cl pH 7.5, 5 mM MgCl$_2$, 50 mM KCl,

1 mM DTT, 2.5% glycerol, and 0.5% NP-40), 50 ng/ml poly dI•dC, 40 fmol biotinylated oligonucleotides (IDT). The reactions were then allowed to sit on ice for 5 min, then at room temperature for 15 min. The reactions were then loaded onto a pre-run 6% TBE polyacrylamide gel followed by transfer to a Biodyne B positively charged membrane (Pall life sciences, 60208). Membranes were developed using a Light Shift chemiluminescent EMSA kit (Thermo Scientific, 20148).

Recombinant protein expression and purification

GST and His-tagged protein expression constructs were expressed and purified as previously described (11). Protein expression was induced with 1 mM IPTG and cells were collected 3 to 4 h later. All constructs except for the His-tagged mutant SOX9 HMG were grown using the BL21(DE3) *Escherichia coli* strain (Thermo Scientific, EC0114). The mutant HMG construct was expressed and purified in the Rosetta(DE3) strain (Novagen, 70954).

GST pull-down assays

The concentration of purified recombinant proteins was measured using Bradford's reagent (Bio-Rad, 5000202). About 0.25 to 2 μg of each protein was used in a binding reaction. Binding reactions were carried out in a binding buffer containing 25 mM Hepes pH 7.5, 12.5 mM MgCl2, 300 mM KCl, 0.1% NP-40, 1 mg/ml bovine serum albumin, 1 mM DTT. GST and His-tagged proteins were mixed in binding buffer to a total volume of 200 μl and incubated in a rotator for 1 h at 4 °C. Glutathione-sepharose (Thermo-Scientific, 25236) were washed thrice in binding buffer and then added to binding reactions at a packed bead volume of 10 μl per reaction. After another 1 h incubation at 4 °C with rotation, beads were washed thrice in washing buffer (25 mM Hepes pH 7.5, 12.5 mM MgCl2, 400 mM KCl, 0.5% NP-40) and eluted by boiling for 5 min in 2× SDS buffer (100 mM Tris-Cl pH 6.8, 4% SDS, 0.2% bromophenol blue, 20% glycerol). Samples were then analyzed by SDS-PAGE followed by Western blotting.

Western blotting

Western blotting was performed after SDS-PAGE as previously described (11). Western blots were probed with the following antibodies: anti-Flag-HRP (Sigma–Aldrich, A8592), anti-SOX9 (Sigma–Aldrich, AB5535), anti-β-catenin (BD Biosciences, 610154), anti-β-tubulin (Proteintech, 66240-1-Ig), anti-His (Cytiva, 27-4710-01).

Protein structure visualization

Protein structures were downloaded from RSC PDB and visualized with UCSF ChimeraX (76), developed by the Resource for Biocomputing, Visualization, and Informatics at the University of California, San Francisco, with support from National Institutes of Health R01-GM129325 and the Office of Cyber Infrastructure and Computational Biology, National Institute of Allergy and Infectious Diseases.

Data collection and analysis

Cell culture experiments were performed in biological triplicates. Cells in different wells or plates were independently treated with drugs or transfected as indicated for each experiment and subsequently assayed independently. To ensure reproducibility, all experiments were repeated at least three different times with similar results. Data were then analyzed and graphed using Graphpad Prism 9 (GraphPad Software Inc). The specific statistical tests used to calculate p-values are indicated in the figure legends.

Data availability

The data supporting the findings in this study are available within the article and supplemental information. All reagents described in this study are available upon request.

References

1. Clevers, H., Loh, K. M., and Nusse, R. (2014) An integral program for tissue renewal and regeneration: Wnt signaling and stem cell control. *Science* **346**, 1248012
2. Ramakrishnan, A.-B., and Cadigan, K. M. (2017) Wnt target genes and where to find them. *F1000Res* **6**, 746

3. Archbold, H. C., Yang, Y. X., Chen, L., and Cadigan, K. M. (2012) How do they do Wnt they do?: regulation of transcription by the Wnt/β-catenin pathway. *Acta Physiol.* **204**, 74–109

4. Clevers, H., and Nusse, R. (2012) Wnt/β-Catenin signaling and disease. *Cell* **149**, 1192–1205

5. Acebron, S. P., and Niehrs, C. (2016) β-Catenin-Independent roles of Wnt/LRP6 signaling. *Trends Cell Biol.* **26**, 956–967

6. Yang, Y., and Mlodzik, M. (2015) Wnt-frizzled/planar cell polarity signaling: cellular orientation by facing the wind (Wnt). *Annu. Rev. Cell Dev. Biol.* **31**, 623–646

7. Nakamura, Y., and Hoppler, S. (2017) Genome-wide analysis of canonical Wnt target gene regulation in Xenopus tropicalis challenges β-catenin paradigm. *genesis* **55**, e22991

8. Söderholm, S., and Cantù, C. (2021) The WNT/β-catenin dependent transcription: a tissue-specific business. *WIREs Mech. Dis.* **13**, e1511

9. Lewis, A., Freeman-Mills, L., de la Calle-Mustienes, E., Giráldez-Pérez, R. M., Davis, H., Jaeger, E., *et al.* (2014) A polymorphic enhancer near GREM1 influences bowel cancer risk through differential CDX2 and TCF7L2 binding. *Cell Rep.* **8**, 983–990

10. Verzi, M. P., Hatzis, P., Sulahian, R., Philips, J., Schuijers, J., Shin, H., *et al.* (2010) TCF4 and CDX2, major transcription factors for intestinal function, converge on the same cis-regulatory regions. *Proc. Natl. Acad. Sci. U. S. A.* **107**, 15157–15162

11. Ramakrishnan, A.-B., Chen, L., Burby, P. E., and Cadigan, K. M. (2021) Wnt target enhancer regulation by a CDX/TCF transcription factor collective and a novel DNA motif. *Nucl. Acids Res.* **49**, 8625–8641

12. Kormish, J. D., Sinner, D., and Zorn, A. M. (2010) Interactions between SOX factors and Wnt/β-catenin signaling in development and disease. *Dev. Dyn.* **239**, 56–68

13. Sinner, D., Kordich, J. J., Spence, J. R., Opoka, R., Rankin, S., Lin, S.-C. J., *et al.* (2007) Sox17 and Sox4 differentially regulate β-catenin/T-cell factor Activity and proliferation of colon carcinoma cells. *Mol. Cell. Biol.* **27**, 7802–7815

14. Mukherjee, S., Chaturvedi, P., Rankin, S. A., Fish, M. B., Wlizla, M., Paraiso, K. D., *et al.* (2020) Sox17 and β-catenin co-occupy Wnt-responsive enhancers to govern the endoderm gene regulatory network. *eLife* **9**, e58029

15. Mukherjee, S., Luedeke, D. M., McCoy, L., Iwafuchi, M., and Zorn, A. M. (2022) SOX transcription factors direct TCF-independent WNT/β-catenin responsive transcription to govern cell fate in human pluripotent stem cells. *Cell Rep* **40**, 111247

16. Lefebvre, V. (2019) Seven - roles and regulation of SOX transcription factors in skeletogenesis. In: *Current Topics in Developmental Biology. Vertebrate Skeletal Development*, B. R. Olsen, editor. Academic Press, Cambridge, MA. **133**, 171–193

17. Lefebvre, V., Angelozzi, M., and Haseeb, A. (2019) SOX9 in cartilage development and disease. *Curr. Opin. Cell Biol.* **61**, 39–47

18. Sekido, R., and Lovell-Badge, R. (2008) Sex determination involves synergistic action of SRY and SF1 on a specific Sox9 enhancer. *Nature* **453**, 930–934

19. Nicol, B., and Yao, H. H.-C. (2015) Gonadal identity in the absence of pro-testis factor SOX9 and pro-ovary factor beta-catenin in Mice1. *Biol. Reprod.* **93**, 1–12

20. Akiyama, H., Lyons, J. P., Mori-Akiyama, Y., Yang, X., Zhang, R., Zhang, Z., *et al.* (2004) Interactions between Sox9 and β-catenin control chondrocyte differentiation. *Genes Dev.* **18**, 1072–1087

21. Sellak, H., Wu, S., and Lincoln, T. M. (2012) KLF4 and SOX9 transcription factors antagonize β-catenin and inhibit TCF-activity in cancer cells. *Biochim. Biophys. Acta (Bba) - Mol. Cell Res.* **1823**, 1666–1675

22. Sinha, A., Fan, V. B., Ramakrishnan, A.-B., Engelhardt, N., Kennell, J., and Cadigan, K. M. (2021) Repression of Wnt/β-catenin signaling by SOX9 and Mastermind-like transcriptional coactivator 2. *Sci. Adv.* **7**, eabe0849

23. Topol, L., Chen, W., Song, H., Day, T. F., and Yang, Y. (2009) Sox9 inhibits Wnt signaling by promoting β-catenin phosphorylation in the nucleus. *J. Biol. Chem.* **284**, 3323–3333

24. van Es, J. H., Jay, P., Gregorieff, A., van Gijn, M. E., Jonkheer, S., Hatzis, P., *et al.* (2005) Wnt signalling induces maturation of Paneth cells in intestinal crypts. *Nat. Cell Biol.* **7**, 381–386

25. van Es, J. H., Haegebarth, A., Kujala, P., Itzkovitz, S., Koo, B.-K., Boj, S. F., *et al.* (2012) A critical role for the Wnt effector Tcf4 in adult intestinal homeostatic self-renewal. *Mol. Cell Biol.* **32**, 1918–1927

26. Blache, P., van de Wetering, M., Duluc, I., Domon, C., Berta, P., Freund, J.-N., *et al.* (2004) SOX9 is an intestine crypt transcription factor, is regulated by the Wnt pathway, and represses the CDX2 and MUC2 genes. *J. Cell Biol.* **166**, 37–47

27. Bastide, P., Darido, C., Pannequin, J., Kist, R., Robine, S., Marty-Double, C., *et al.* (2007) Sox9 regulates cell proliferation and is required for Paneth cell differentiation in the intestinal epithelium. *J. Cell Biol.* **178**, 635–648

28. Mori–Akiyama, Y., van den Born, M., van Es, J. H., Hamilton, S. R., Adams, H. P., Zhang, J., *et al.* (2007) SOX9 is required for the differentiation of Paneth cells in the intestinal epithelium. *Gastroenterology* **133**, 539–546

29. Liang, X., Duronio, G. N., Yang, Y., Bala, P., Hebbar, P., Spisak, S., *et al.* (2022) An enhancer-driven stem cell–like program mediated by SOX9 blocks intestinal differentiation in colorectal cancer. *Gastroenterology* **162**, 209–222

30. Wehkamp, J., Wang, G., Kübler, I., Nuding, S., Gregorieff, A., Schnabel, A., *et al.* (2007) The Paneth cell α-defensin deficiency of ileal crohn's disease is linked to Wnt/Tcf-4. *J. Immunol.* **179**, 3109–3118

31. Beisner, J., Teltschik, Z., Ostaff, M. J., Tiemessen, M. M., Staal, F. J. T., Wang, G., *et al.* (2014) TCF-1-mediated Wnt signaling regulates Paneth cell innate immune defense effectors HD-5 and -6: Implications for crohn's disease. *Am. J. Physiol. - Gastrointest. Liver Physiol.* **307**, G487–G498

32. Gregorieff, A., and Clevers, H. (2005) Wnt signaling in the intestinal epithelium: From endoderm to cancer. *Genes Dev.* **19**, 877–890

33. Dave, K., Sur, I., Yan, J., Zhang, J., Kaasinen, E., Zhong, F., *et al.* (2017) Mice deficient of Myc super-enhancer region reveal differential control mechanism between normal and pathological growth. *eLife* **6**, e23382

34. Konsavage, W. M., and Yochum, G. S. (2014) The myc 3' Wnt-responsive element suppresses colonic tumorigenesis. *Mol. Cell. Biol.* **34**, 1659–1669

35. Tuupanen, S., Turunen, M., Lehtonen, R., Hallikas, O., Vanharanta, S., Kivioja, T., *et al.* (2009) The common colorectal cancer predisposition SNP rs6983267 at chromosome 8q24 confers potential to enhanced Wnt signaling. *Nat. Genet.* **41**, 885–890

36. Wright, J. B., Brown, S. J., and Cole, M. D. (2010) Upregulation of c-MYC in cis through a large chromatin loop linked to a cancer risk-associated single-nucleotide polymorphism in colorectal cancer cells. *Mol. Cell. Biol.* **30**, 1411–1420

37. Matheu, A., Collado, M., Wise, C., Manterola, L., Cekaite, L., Tye, A. J., *et al.* (2012) Oncogenicity of the developmental transcription factor Sox9. *Cancer Res.* **72**, 1301–1315

38. Prévostel, C., and Blache, P. (2017) The dose-dependent effect of SOX9 and its incidence in colorectal cancer. *Eur. J. Cancer* **86**, 150–157

39. Xu, Y., Zhang, X., Hu, X., Zhou, W., Zhang, P., Zhang, J., *et al.* (2018) The effects of lncRNA MALAT1 on proliferation, invasion and migration in colorectal cancer through regulating SOX9. *Mol. Med.* **24**, 52

40. Zhou, T., Wu, L., Ma, N., Tang, F., Yu, Z., Jiang, Z., *et al.* (2020) SOX9-activated FARSA-AS1 predetermines cell growth, stemness, and metastasis in colorectal cancer through upregulating FARSA and SOX9. *Cell Death Dis.* **11**, 1–15

41. van de Wetering, M., Oving, I., Muncan, V., Fong, M. T. P., Brantjes, H., Leenen, D. van, *et al.* (2003) Specific inhibition of gene expression using a stably integrated, inducible small-interfering-RNA vector. *EMBO Rep.* **4**, 609–615

42. Li, V. S. W., Ng, S. S., Boersema, P. J., Low, T. Y., Karthaus, W. R., Gerlach, J. P., *et al.* (2012) Wnt signaling through inhibition of β-catenin degradation in an intact Axin1 complex. *Cell* **149**, 1245–1256

43. Kishida, S., Yamamoto, H., Ikeda, S., Kishida, M., Sakamoto, I., Koyama, S., *et al.* (1998) Axin, a negative regulator of the Wnt signaling pathway, directly interacts with adenomatous polyposis coli and regulates the stabilization of β-catenin*. *J. Biol. Chem.* **273**, 10823–10826

44. van de Wetering, M., Sancho, E., Verweij, C., de Lau, W., Oving, I., Hurlstone, A., *et al.* (2002) The β-catenin/TCF-4 complex imposes a crypt progenitor phenotype on colorectal cancer cells. *Cell* **111**, 241–250

45. Barretina, J., Caponigro, G., Stransky, N., Venkatesan, K., Margolin, A. A., Kim, S., *et al.* (2012) The Cancer Cell Line Encyclopedia enables predictive modelling of anticancer drug sensitivity. *Nature* **483**, 603–607

46. Ghandi, M., Huang, F. W., Jané-Valbuena, J., Kryukov, G. V., Lo, C. C., McDonald, E. R., *et al.* (2019) Next-generation characterization of the cancer cell line Encyclopedia. *Nature* **569**, 503–508

47. Dempster, J. M., Boyle, I., Vazquez, F., Root, D. E., Boehm, J. S., Hahn, W. C., *et al.* (2021) Chronos: a cell population dynamics model of CRISPR experiments that improves inference of gene fitness effects. *Genome Biol.* **22**, 343

48. Van der Flier, L. G., Sabates–Bellver, J., Oving, I., Haegebarth, A., De Palo, M., Anti, M., *et al.* (2007) The intestinal Wnt/TCF signature. *Gastroenterology* **132**, 628–632

49. Tomlinson, I., Webb, E., Carvajal-Carmona, L., Broderick, P., Kemp, Z., Spain, S., *et al.* (2007) A genome-wide association scan of tag SNPs identifies a susceptibility variant for colorectal cancer at 8q24.21. *Nat. Genet.* **39**, 984–988

50. Zanke, B. W., Greenwood, C. M., Rangrej, J., Kustra, R., Tenesa, A., Farrington, S. M., *et al.* (2007) Genome-wide association scan identifies a colorectal cancer susceptibility locus on chromosome 8q24. *Nat. Genet.* **39**, 989–994

51. Shi, Z., Chiang, C.-I., Labhart, P., Zhao, Y., Yang, J., Mistretta, T.-A., *et al.* (2015) Context-specific role of SOX9 in NF-Y mediated gene regulation in colorectal cancer cells. *Nucl. Acids Res.* **43**, 6257–6269

52. Coustry, F., Oh, C., Hattori, T., Maity, S. N., Crombrugghe, B. de, and Yasuda, H. (2010) The dimerization domain of SOX9 is required for transcription activation of a chondrocyte-specific chromatin DNA template. *Nucl. Acids Res.* **38**, 6018–6028

53. Sotelo, J., Esposito, D., Duhagon, M. A., Banfield, K., Mehalko, J., Liao, H., *et al.* (2010) Long-range enhancers on 8q24 regulate c-Myc. *Proc. Natl. Acad. Sci. U. S. A.* **107**, 3001–3005

54. Yochum, G. S., Cleland, R., and Goodman, R. H. (2008) A genome-wide screen for β-catenin binding sites identifies a downstream enhancer element that controls c-myc gene expression. *Mol. Cell Biol.* **28**, 7368–7379

55. Yochum, G. S., Sherrick, C. M., MacPartlin, M., and Goodman, R. H. (2010) A β-catenin/TCF-coordinated chromatin loop at MYC integrates 5′ and 3′ Wnt responsive enhancers. *Proc. Natl. Acad. Sci. U. S. A.* **107**, 145–150

56. Coste, A. de L., Romagnolo, B., Billuart, P., Renard, C.-A., Buendia, M.-A., Soubrane, O., *et al.* (1998) Somatic mutations of the β-catenin gene are frequent in mouse and human hepatocellular carcinomas. *Proc. Natl. Acad. Sci. U. S. A.* **95**, 8847–8851

57. Dietinger, V., García de Durango, C. R., Wiechmann, S., Boos, S. L., Michl, M., Neumann, J., *et al.* (2020) Wnt-driven LARGE2 mediates laminin-adhesive O-glycosylation in human colonic epithelial cells and colorectal cancer. *Cell Commun. Signal.* **18**, 102

58. Stamos, J. L., and Weis, W. I. (2013) The β-catenin destruction complex. *Cold Spring Harb. Perspect. Biol.* **5**, a007898

59. Molenaar, M., van de Wetering, M., Oosterwegel, M., Peterson-Maduro, J., Godsave, S., Korinek, V., *et al.* (1996) XTcf-3 transcription factor mediates β-catenin-induced Axis formation in Xenopus embryos. *Cell* **86**, 391–399

60. Cadigan, K. M., and Waterman, M. L. (2012) TCF/LEFs and Wnt signaling in the nucleus. *Cold Spring Harb. Perspect. Biol.* **4**, a007906

61. Abdel-Samad, R., Zalzali, H., Rammah, C., Giraud, J., Naudin, C., Dupasquier, S., *et al.* (2011) MiniSOX9, a dominant-negative variant in colon cancer cells. *Oncogene* **30**, 2493–2503

62. Patil, A., Hughes, A. L., and Zhang, G. (2004) Rapid evolution and diversification of mammalian α-defensins as revealed by comparative analysis of rodent and primate genes. *Physiol. Genomics* **20**, 1–11

63. Bernard, P., Tang, P., Liu, S., Dewing, P., Harley, V. R., and Vilain, E. (2003) Dimerization of SOX9 is required for chondrogenesis, but not for sex determination. *Hum. Mol. Genet.* **12**, 1755–1765

64. Sato, T., van Es, J. H., Snippert, H. J., Stange, D. E., Vries, R. G., van den Born, M., *et al.* (2011) Paneth cells constitute the niche for Lgr5 stem cells in intestinal crypts. *Nature* **469**, 415–418

65. Roche, K. C., Gracz, A. D., Liu, X. F., Newton, V., Akiyama, H., and Magness, S. T. (2015) SOX9 maintains reserve stem cells and preserves radioresistance in mouse small intestine. *Gastroenterology* **149**, 1553–1563.e10

66. Nusse, R. (2005) Wnt signaling in disease and in development. *Cell Res.* **15**, 28–32

67. Nusse, R., and Clevers, H. (2017) Wnt/β-Catenin signaling, disease, and emerging therapeutic modalities. *Cell* **169**, 985–999

68. Polakis, P. (2012) Wnt signaling in cancer. *Cold Spring Harb. Perspect. Biol.* **4**, a008052

69. Baar, M. P., Brandt, R. M. C., Putavet, D. A., Klein, J. D. D., Derks, K. W. J., Bourgeois, B. R. M., *et al.* (2017) Targeted apoptosis of senescent cells restores tissue homeostasis in response to chemotoxicity and aging. *Cell* **169**, 132–147.e16

70. Schuijers, J., Mokry, M., Hatzis, P., Cuppen, E., and Clevers, H. (2014) Wnt-induced transcriptional activation is exclusively mediated by TCF/LEF. *EMBO J.* **33**, 146–156

71. Schindelin, J., Arganda-Carreras, I., Frise, E., Kaynig, V., Longair, M., Pietzsch, T., *et al.* (2012) Fiji: an open-source platform for biological-image analysis. *Nat. Met.* **9**, 676–682

72. Nix, D. A., Courdy, S. J., and Boucher, K. M. (2008) Empirical methods for controlling false positives and estimating confidence in ChIP-Seq peaks. *BMC Bioinform.* **9**, 523

73. Lopez-Delisle, L., Rabbani, L., Wolff, J., Bhardwaj, V., Backofen, R., Grüning, B., *et al.* (2021) pyGenomeTracks: reproducible plots for multivariate genomic datasets. *Bioinformatics* **37**, 422–423

74. Grant, C. E., Bailey, T. L., and Noble, W. S. (2011) Fimo: scanning for occurrences of a given motif. *Bioinformatics* **27**, 1017–1018

75. Fornes, O., Castro-Mondragon, J. A., Khan, A., van der Lee, R., Zhang, X., Richmond, P. A., *et al.* (2020) Jaspar 2020: Update of the open-access database of transcription factor binding profiles. *Nucl. Acids Res.* **48**, D87–D92

76. Pettersen, E. F., Goddard, T. D., Huang, C. C., Meng, E. C., Couch, G. S., Croll, T. I., *et al.* (2021) UCSF ChimeraX: structure visualization for researchers, educators, and developers. *Protein Sci.* **30**, 70–82

ASBMB